2014 IEEE International Conference on Robotics & Automation (ICRA)
Hong Kong Convention and Exhibition Center
May 31 - June 7, 2014. Hong Kong, China

Two-finger Caging of 3D Polyhedra Using Contact Space Search

Thomas F. Allen[1], Elon Rimon[2], and Joel W. Burdick[1]

Abstract— **Multi-finger caging offers a robust approach to grasping. This paper describes an algorithm to find caging formations of a 3D polyhedron for two point fingers using a lower-dimensional contact-space formulation. The paper shows that contact space has several useful properties. First, the critical points of the cage in the hand's configuration space are identical to the critical points of the interfinger distance in contact space. Second, contact space can be naturally decomposed into 4D regions having useful properties. A geometric analysis of the critical points of the interfinger distance function results in a catalog of grasps in which the cages change topology, leading to a simple test to classify critical points. These properties lead to an easily constructed *caging graph* whose nodes contain the critical points of contact space. Starting from an immobilizing grasp, this graph can be searched to find local, intermediate, and maximal caging regions around that initial grasp. An implemented algorithm demonstrates the method.**

I. Introduction

An object surrounded by fingers such that it may have some local freedom but cannot escape to infinity is said to be *caged*. Caging is a promising method for adding robustness to robotic grasping. If a robot places its fingers in a caging formation around the object to be grasped, the robot can robustly close its fingers without the object falling out of the hand. This paper presents an algorithm for caging a 3D polyhedron using two point fingers, based on a contact-space formulation.

Introduced to robotics by Rimon and Blake [1], [2], caging has become an important part of grasping research. Sudsang and Ponce [3], as well as many others [4], [5], [6], [7], [8] have presented algorithms for two-finger caging of 2D polygons. Vahedi and van der Stappen [9] presented comprehensive caging sets for two fingers and some solutions for three fingers. More recent work includes [6], [10], [11].

Several works by Pipattansomporn et al [12], [13] have examined caging of 3D polyhedra. The contact-space formulation presented in this paper allows most of the computation to be done in the 4D contact space, rather than the object's 6D configuration space. This approach leads to an algorithm which is simple to implement and has sound computation efficiency. The search algorithm, but not the analysis, is very similar to one presented for 2D polygons by these same authors [14]. Because the 2D analysis is much simpler, but the resulting algorithm is similar, it may be helpful to review that paper before proceeding.

The algorithm presented in this paper takes as starting input a 3D polyhedron and an initial immobilizing grasp. Starting with that grasp, it searches a graph composed of critical points of the interfinger distance function. It reports the local, intermediate, and maximal caging sets related to this immobilizing grasp.

Note that two point fingers cannot immobilize a polyhedron, as it will always be able to rotate about a line passing through both fingers. However, the two-fingered hand is immobilizing relative to the object. In this paper, immobilizing refers to this situation.

This paper is organized as follows. Section II defines the problem and introduces the interfinger distance function, $d(\mathbf{s})$. Section III reformulates the 6D caging problem into 4D contact space. Section IV introduces a discrete caging graph, G, whose nodes will be searched using the algorithm presented in Section V. An example in Section VI demonstrates the algorithm. Section VII presents a geometric method to characterize all nodes of G, which results in a catalog of all squeezing, immobilizing, and puncture grasps, shown in Section VIII. In certain cases, important information is lost when moving from configuration space to contact space. Section IX shows when information is lost and how to restore it, such that the search algorithm is correct.

II. Preliminaries and Problem Statement

A 3D polyhedral object, $\mathcal{B}$, is to be caged by two point fingers, denoted f_1 and f_2. The polyhedron may not have cavities in its interior, but may have holes passing through it. Two-finger cages come in two types: *squeezing* cages, where the fingers move together to cage the object and *stretching* cages, where the fingers move apart to cage the object [9], [6]. This paper considers only squeezing cages. To simplify the explanation, we exclude polyhedra containing parallel opposing faces, parallel opposing edges, and edges and faces which are parallel and not coplanar, though the algorithm can handle these cases. Non-convex faces of $\mathcal{B}$ must be divided into a disjoint collection of convex faces.

Definition 1: The **configuration space** (c-space) of a two-fingered hand, denoted $\mathcal{C}$, is the 6D space consisting of configurations $q = (p_1, p_2) \in \mathbb{R}^6$, where $p_i = (x_i, y_i, z_i) \in \mathbb{R}^3$ represents the position of the i^{th} finger, for $i = 1, 2$.

From the hand's point of view, the object $\mathcal{B}$ forms an obstacle. The *c-space obstacle* corresponding to $\mathcal{B}$, denoted $\mathcal{CB}$, is the set of hand configurations at which one or both

This work was performed for the Jet Propulsion Laboratory, California Institute of Technology, with funding from the DARPA Autonomous Robotic Manipulation Software Track (ARM-S) and the U.S. Army under the Robotics Collaborative Technology Alliance through an agreement with the National Aeronautics and Space Administration.

[1]Thomas F. Allen and Joel W. Burdick are with the Department of Mechanical Engineering, California Institute of Technology, Pasadena, California, USA. tallen@caltech.edu, jwb@robotics.caltech.edu

[2]Elon Rimon is with the Department of Mechanical Engineering, Israel Institute of Technology, Hiafa, Israel. rimon@technion.ac.il

fingers intersect the stationary object $\mathcal{B}$. The hand's *free c-space,* $\mathcal{F}$, is the complement of $\mathcal{CB}$'s interior. The boundary of $\mathcal{F}$ consists of all hand configurations at which one or both fingers touch the object's boundary.

Our approach is formulated in contact space.

Definition 2: **Contact-space**, denoted $\mathcal{U}$, consists of all hand configurations at which both fingers touch the object boundary. Contact space is a 4-dimensional submanifold of $\mathcal{C}$, lying on the boundary of $\mathcal{F}$.

Since the position of one finger on the surface of $\mathcal{B}$ may be parameterized using a subset of $\mathbb{R}^2$, $\mathcal{U}$ may be parameterized as a subset of $\mathbb{R}^4$. Denote a point in contact space with $\mathbf{s} = (s_1, s_2, s_3, s_4) \in \mathbb{R}^4$. For any point $\mathbf{s} \in \mathcal{U}$, the corresponding finger positions in $\mathcal{C}$ may be given by $q(\mathbf{s}) = (p_1(s_1, s_2), p_2(s_3, s_4))$. Note that implementation of this parameterization is not required for our caging algorithm.

Contact space can be naturally decomposed into a set of polychora (4-polytopes), which provide a useful structure to calculate caging sets.

Definition 3: A **contact-space polychoron**, $\mathcal{P}_{ij}$ corresponds to all possible placements of f_1 at $p_1(s_1, s_2)$ on face i and f_2 at $p_2(s_3, s_4)$ on face j of $\mathcal{B}$.

Each polychoron, $\mathcal{P}_{ij}$, is a convex set. The set of polychora completely covers contact space and their interiors are disjoint. The following definition will be critical to the consideration of caging.

Definition 4: The **interfinger distance function** is a scalar valued function giving the distance between the fingers. In $\mathcal{C}$, $d : \mathcal{C} \to \mathbb{R}$ and in $\mathcal{U}$, $d : \mathcal{U} \to \mathbb{R}$.

$$d(q) = d(p_1, p_2) = ||p_1 - p_2|| \quad (1)$$

$$d(\mathbf{s}) = ||p_1(s_1, s_2) - p_2(s_1, s_2)|| \quad (2)$$

The notion of a *caging set* is formulated in $\mathcal{F}$ as follows.

Definition 5: The **caging set** of $\mathcal{B}$ consists of all pairs of finger placements in $\mathcal{F}$ such that $\mathcal{B}$ cannot be moved arbitrarily far from the fingers.

Definition 6: A **squeezing caging set** of $\mathcal{B}$ is any pair of finger placements, $q_0 \in \mathcal{F}$, such that $\mathcal{B}$ cannot be moved arbitrarily far from the fingers while the interfinger distance is constrained such that $d(q) \geq d(q_0)$.

When two fingers initially holding $\mathcal{B}$ at an immobilizing grasp are moved apart, the object remains caged for a finite range of the finger opening distance. Eventually the interfinger distance reaches a critical value beyond which the object can escape the cage formed by the two fingers. This critical finger opening may only allow an intermediate escape into a larger cage formed by other object features, or an ultimate escape to infinity. We propose to find those critical events by searching contact space, $\mathcal{U}$.

Problem Definition: Given an initial two-finger immobilizing grasp of $\mathcal{B}$, compute the following types of caging set:

1) The *initial caging set*—the largest caging set from which the fingers are guaranteed to return to the initial immobilizing grasp while keeping the object caged during the squeezing process.
2) The *intermediate caging set*—any caging set which contains the initial caging set, such that all fingers end at a finite number of possible immobilizing grasps while keeping the object caged during a squeeze.
3) The *maximal caging set*—the largest squeezing caging set which contains the initial caging set.

III. Contact-Space Reformulation of Caging

Rather than searching configuration space, $\mathcal{C} \in \mathbb{R}^6$, this paper reduces the dimensionality of the problem by searching contact space, $\mathcal{U} \subset \mathbb{R}^4$. To show that a search in $\mathcal{U}$ can find the caging sets, we formulate the caging problem as the existence of a test path between two points lying entirely in a sublevel set of the function $d(\mathbf{s})$ in $\mathcal{U}$.

The idea of an *escape* plays a central role in caging theory. The standard definition of an escape is the ability to move the two-fingered hand with a fixed finger opening arbitrarily far from the object. The corresponding notion of an *escape* in contact space is defined as follows.

Definition 7: A **contact-space escape point** in $\mathcal{U}$ is any point where the fingers are coincident on the boundary of a contact-space polychoron. We denote this as $\Delta = \{\mathbf{s} \in \mathcal{U} \mid p_1(s_1, s_2) = p_2(s_3, s_4)\}$.

The notion of a contact-space escape point in $\mathcal{U}$ is equivalent to the standard definition of an escape as follows. Upon reaching a contact-space escape point, the two fingers are coincident and can move arbitrarily far from $\mathcal{B}$. Conversely, suppose the hand can move arbitrarily far from $\mathcal{B}$ according to the standard definition of escape. The two fingers can be moved to be coincident, then moved back to the object's boundary, which is an escape point in $\mathcal{U}$. Every contact-space escape point in $\mathcal{U}$ has an equivalent point in $\mathcal{F}$.

A *c-sublevel set* of $d(\mathbf{s})$ in contact space is the set $\mathcal{U}_{\leq c} = \{\mathbf{s} \in \mathbb{R}^4 : d(\mathbf{s}) \leq c\}$. Similarly, a c-sublevel set of $d(q)$ in the free c-space is the set $\mathcal{F}_{\leq c} = \{q \in \mathbb{R}^6 : d(q) \leq c\}$.

Definition 8: A **c-sublevel path** in $\mathcal{F}$ or $\mathcal{U}$ is a path along which the maximum value of the inter-finger distance does not exceed c.

Thus, an object is caged for interfinger distance σ^* if and only if there does not exist a σ^*-sublevel path in $\mathcal{F}$ from its current configuration to an escape point.

Let the object $\mathcal{B}$ be initially immobilized at a hand configuration q_0. For a certain interval of finger openings, $[\sigma_0, \sigma_1)$, where $\sigma_0 = d(q_0)$, the object remains caged by the two fingers. The cage is broken at a hand configuration, q_1, where $\sigma_1 = d(q_1) > \sigma_0$. This grasp is referred to as a *join point*, *puncture point*, or *puncture grasp.* Starting at the immobilizing grasp q_0, the value of σ at the *first* puncture point can be viewed as the minimum value, σ_1, such that a σ_1-sublevel path exists between q_0 and either an escape point or another immobilizing grasp. The value of σ at the *last* puncture point can be viewed as the minimum value, σ_{max}, such that a σ_{max}-sublevel path exists between q_0 and an escape point.

IV. The Caging Graph

Rather than searching the continuous spaces $\mathcal{F}$ or $\mathcal{U}$, we show below that only a discrete set of points must be searched. This set of points form nodes in the *caging graph*, denoted G, which captures the topology of the sublevel sets of $d(\mathbf{s})$ in $\mathcal{U}$. The graph will be the basis for the algorithm described in Section V.

A. Location of Important Grasps

Rimon and Blake [2] showed that immobilizing and puncture grasps occur only at frictionless equilibrium grasps. For a polyhedron, excluding non-generic parallel geometry, frictionless equilibrium grasps only occur at a finite, discrete set of points, corresponding to finger pairs touching vertices, edges, or faces. The combinations of contact pairs which may result in frictionless equilibrium grasps are:

1) a *vertex-vertex* pair
2) a *vertex-edge* pair, with one finger touching an edge at the point where the perpendicular projection of the vertex onto that edge lies
3) a *vertex-face* pair, with one finger touching a face at the point where the perpendicular projection of the vertex onto that face lies
4) an *edge-edge* pair, in which the fingers lie at points corresponding to the unique minimum distance between those two lines, such that a line connecting the two points is perpendicular to both edges

For cases 2-4, the point may not exist for a specific pair, if the location of either finger does not lie on the interior of its associated edge or face. These points will form the nodes of a *caging graph*, defined below. They are exactly the critical points of the inter-finger distance function, $d(\mathbf{s})$, in $\mathcal{U}$. Note that because contacts both lying on faces of the polyhedron do not form frictionless equilibrium grasps (as parallel faces are excluded), all these points lie on the *boundaries* of contact-space polychora.

Definition 9: The **caging graph**, G, is an undirected graph with the following nodes and edges:
Nodes: The nodes of G correspond to all critical points of the interfinger distance function in $\mathcal{U}$. In particular, they are all vertex-vertex pairs, and the unique local minimum associated with each vertex-edge, vertex-face, and edge-edge pair, if that minimum exists.
Edges: All nodes lying on the boundary of the *same* contact-space polychoron, $\mathcal{P}_{ij}$, are connected to each other by edges in G.

Because we propose to search the caging grasps, G, rather than free c-space, $\mathcal{F}$, we must justify that the two searches will produce the same result. To that end we introduce the notion of *sublevel set equivalence*.

Definition 10: Contact space, $\mathcal{U}$, is **sublevel equivalent** with the free c-space, $\mathcal{F}$, if the following holds: for any two points $q, q' \in \mathcal{U}$ there exists a c-sublevel path between q and q' in $\mathcal{U}$ if and only if there exists a c-sublevel path between their equivalent points in $\mathcal{F}$.

Similarly, G and $\mathcal{U}$ are sublevel equivalent if, for any two nodes, $q, q' \in G$ there exists a c-sublevel path between q and q' in G if and only if there exists a c-sublevel path between their equivalent points in $\mathcal{U}$.

The caging graph, G, and contact space, $\mathcal{U}$ are always sublevel equivalent. The proof is delayed until Sec. IX. For many objects, $\mathcal{U}$ and $\mathcal{F}$ are sublevel equivalent. However, for some objects, they are not. For such objects we must perform a rigorous characterization of the critical points of $d(\mathbf{s}) \in \mathcal{U}$, and augment G with a (usually small) number of additional edges. We will proceed assuming that $\mathcal{F}$ and $\mathcal{U}$ are sublevel equivalent, and analyze the case when they are not in Sec. IX.

V. The Caging Algorithm

The caging algorithm is structured as follows. Starting at an immobilizing grasp of $\mathcal{B}$, the algorithm searches the caging graph, G, using two lists of nodes: a list of open nodes, $\mathcal{O}$, and a list of closed nodes, $\mathcal{X}$. The *open list*, $\mathcal{O}$ is kept sorted in ascending order of the associated value of $d(\mathbf{s})$. To start, the node of G associated with the initial immobilizing grasp is marked as open and inserted into $\mathcal{O}$, while $\mathcal{X}$ is initially empty. At each step, the node in $\mathcal{O}$ with the smallest value of $d(\mathbf{s})$ is marked as *current*, removed from $\mathcal{O}$, and added to the *end* of the closed list $\mathcal{X}$. If the $d(\mathbf{s})$ value of the current node is zero, the algorithm halts, as an escape point has been found. Otherwise, each node adjacent to the current node, if it is not already in $\mathcal{X}$ or $\mathcal{O}$, is added to $\mathcal{O}$.

The algorithm's output is extracted from the list $\mathcal{X}$ as discussed below. In particular, the node in $\mathcal{X}$ having the maximal value of $d(\mathbf{s})$ is the *maximal* puncture grasp associated with the initial immobilizing grasp.

A. Analysis of the Closed List

Consider the closed list, $\mathcal{X}$, and index each node, $v \in \mathcal{X}$ in the order it was added. Thus, the first node added (the initial immobilizing grasp), is denoted v_0, and so on. Interfinger distance associated with each node in $\mathcal{X}$, denoted $d(v_i)$, can be seen in Fig. 3.

Definition 11: The i^{th} node, v_i, in the closed list $\mathcal{X}$ is a **local minimum** in $\mathcal{X}$ if $d(v_i) < \min\{d(v_{i-1}), d(v_{i+1})\}$.

Definition 12: The i^{th} node, v_i, in the closed list $\mathcal{X}$ is a **local maximum** in $\mathcal{X}$ if $d(v_i) > \max\{d(v_{i-1}), d(v_{i+1})\}$.

Definition 13: The i^{th} node, v_i, in the closed list $\mathcal{X}$ is a **puncture-related local maximum** if: 1) it is a local maximum of $\mathcal{X}$, and 2) there does not exist a lower-indexed puncture-related local maximum in $\mathcal{X}$, v_j for $j<i$, such that $d(v_j) > d(v_i)$.

The interpretation of the closed list is simple. The first element of $\mathcal{X}$, by construction, and all local minima are immobilizing grasps of $\mathcal{B}$. All puncture-related local maxima are puncture grasps of $\mathcal{B}$. While the node representing this puncture is a saddle of the function $d(\mathbf{s})$ in contact space, $\mathcal{U}$, it appears as a local maximum in $\mathcal{X}$. This occurs because once the search algorithm discovers a saddle, it continues

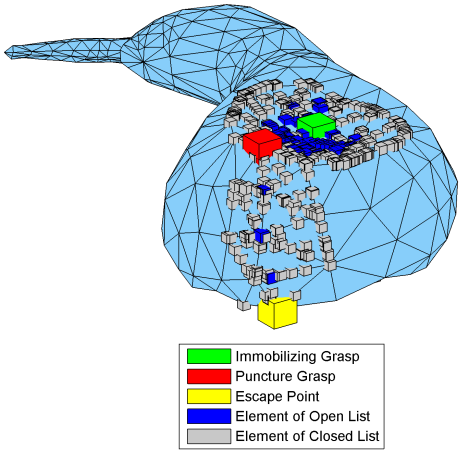

Fig. 1. Exploration of a polyhedron showing finger positions for explored nodes. Note that nodes of G lie in $\mathbb{R}^6$ and cannot be fully visualized in $\mathbb{R}^2$, so pairs of finger positions are shown.

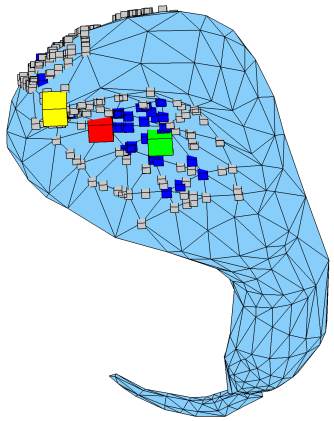

Fig. 2. A second view of the polyhedron.

searching lower-valued nodes in the unexplored portion of the previously disconnected sublevel set of the caging graph, G. The lowest indexed puncture-related local maximum in $\mathcal{X}$ represents the puncture point associated with the local caging set. The highest indexed puncture-related local maximum in $\mathcal{X}$ represents the maximal puncture point associated with the maximal caging set. Finally, all other puncture-related local maxima represent puncture points associated with all intermediate caging sets.

VI. An Example

An example demonstrates the algorithm, searching a polyhedron (modified from [15]) with 326 vertices, 648 faces, and 972 edges. Starting at an immobilizing grasp, the algorithm explores contact space, generating an open list and closed list. Finger positions on $\mathcal{B}$ visited during exploration are shown in Figs. 1 and 2. Interfinger distances associated with nodes of the closed list, $\mathcal{X}$, including the immobilizing and puncture grasps, and the escape point are shown in Fig. 3, plotted against the exploration step of the algorithm. The exploration took 80 steps. Note that only 729 of the 136,632 nodes (0.53%) needed to be checked.

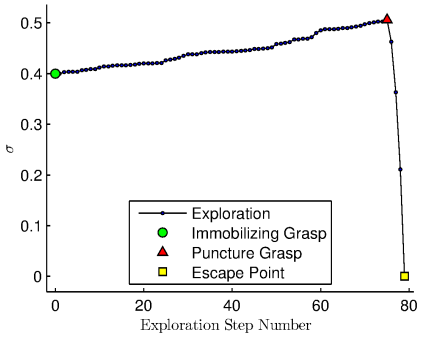

Fig. 3. Interfinger distance of nodes in the closed list, $\mathcal{X}$, vs. exploration step of the algorithm.

VII. Characterization of Nodes of G

In order to establish the sublevel equivalence of free c-space, $\mathcal{F}$, and contact space, $\mathcal{U}$, we must first characterize all points at which the topology of either space may change, which will only occur at nodes of G. Consider a node of G, $q_0 = (p_1^0, p_2^0)$, and its corresponding physical geometry. The following definitions, illustrated by Fig. 4, will help characterize such a node.

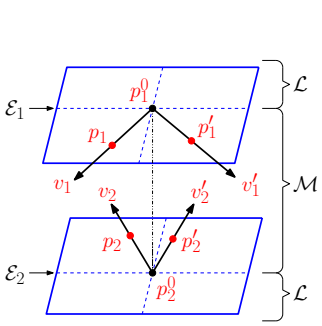

Fig. 4. Geometry used to characterize point $q_0 = (p_1^0, p_2^0)$. Note that no surfaces of $\mathcal{B}$ are shown.

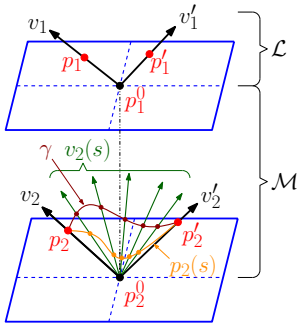

Fig. 5. Construction of a path showing that if $\mathcal{M}_2$ is connected, then D^- is connected.

Definition 14: The **grasp line** for a grasp at $q_0 = (p_1^0, p_2^0)$ is the line segment from p_1^0 to p_2^0 .

Definition 15: The **boundary planes**, denoted $\mathcal{E}_1$, $\mathcal{E}_2$, associated with grasp $q_0 = (p_1^0, p_2^0)$ are two planes perpendicular to the grasp line, passing through p_1^0 and p_2^0, respectively.

Definition 16: The **medial region**, denoted $\mathcal{M}$, associated with grasp $q_0 = (p_1^0, p_2^0)$ is the region lying between $\mathcal{E}_1$ and $\mathcal{E}_2$, not including those planes.

Definition 17: The **lateral region**, denoted $\mathcal{L}$, associated with grasp $q_0 = (p_1^0, p_2^0)$ is the complement of $\mathcal{M}$.

Definition 18: Let $\mathcal{M}_i$ denote the intersection of the $\mathcal{M}$, free physical space, and a ball of radius δ around point p_i^0.

Definition 19: Let $\mathcal{L}_i$ denote the intersection of $\mathcal{L}$, free physical space, and a ball of radius δ around point p_i^0.

The following test characterizes any double contact as an immobilizing grasp, puncture grasp, or neither.

Theorem 1: At a double-contact point, $q_0 = (p_1^0, p_2^0)$, if $\mathcal{M}_1$ and $\mathcal{M}_2$ are both empty, then q_0 is an immobilizing

grasp. If $\mathcal{M}_1$ is empty and $\mathcal{M}_2$ is a path-disconnected set (or $\mathcal{M}_2$ empty and $\mathcal{M}_1$ disconnected), then q_0 is a puncture point. Otherwise, q_0 is neither.

Theorem 1 states that double-contact points may be characterized only by the topology of the regions $\mathcal{M}_1$ and $\mathcal{M}_2$, specifically if each region is the empty set, a path-disconnected set, or a non-empty and path-connected set. Hereafter, disconnected will refer to a path-disconnected set, and connected will refer to a non-empty and path-connected set. The following four cases cover all possible combinations:

1) If $\mathcal{M}_1$ and $\mathcal{M}_2$ are both non-empty (either connected or disconnected), then the topology of sublevel sets of $\mathcal{F}$ do not change at q_0.
2) If $\mathcal{M}_1$ and $\mathcal{M}_2$ are both empty, then q_0 is an immobilizing grasp.
3) If $\mathcal{M}_1$ is empty and $\mathcal{M}_2$ is disconnected (or vice versa), then q_0 is a puncture grasp.
4) If $\mathcal{M}_1$ is empty and $\mathcal{M}_2$ is connected (or vice versa), then the topology of sublevel sets of $\mathcal{F}$ does not change at q_0.

The following characterizations of immobilizing and puncture grasps will be used to analyze the above four cases. Consider a point $q_0 = (p_1^0, p_2^0)$, with $d(q_0) = d_0$. Let D^0 be the slice of $\mathcal{F}$ restricted to $d(q) = d_0$, and let D^- be the slice of $\mathcal{F}$ restricted to $d(q) = d_0 - \epsilon$.

An **immobilizing grasp** at q_0 is characterized locally around q_0 by two criteria:

i. D^- is empty
ii. D^0 is an isolated point

Similarly, a **puncture grasp** is characterized by two criteria:

i. D^- is disconnected
ii. D^0 is connected

To analyze D^- and D^0, consider the following parameterization of a region *in physical space*, in a neighborhood of $q_0 = (p_1^0, p_2^0)$. Let v_i be the vector originating from p_i^0 passing through point p_i, and r_i be the distance from p_i^0 to p_i. Thus, $q = (p_1^0 + r_1 v_1, p_2^0 + r_2 v_2)$. The interfinger distance associated with this point is given by

$$d(q)^2 = d_0^2 + d_0(r_1 v_1^z - r_2 v_2^z) + \mathcal{O}(\mathbf{r}^2) \tag{3}$$

where $d_0 = d(q_0)$ and v_i^z is the z-component of v_i. Note that r_i must be non-negative.

The following geometric insight will also aid in analyzing the above cases. Consider a point p_1^0 on the boundary of $\mathcal{B}$ (which may lie on an edge or at a vertex) and a neighborhood of p_1^0 small enough that no *other* edges or vertices lie in this neighborhood. In this neighborhood, the boundary of $\mathcal{B}$ is formed by one or more planes meeting at p_1^0. Any intersections of those planes also meet at p_1^0. Consider a point, p_1 near p_1^0, and a vector v_1 originating from p_1^0 and passing through p_1, as in Fig. 4. If p_1 lies on the boundary of $\mathcal{B}$, then all points $p_1^0 + \alpha v_1$ for $\alpha \in (0, \delta)$ lie on the boundary $\mathcal{B}$ in some δ-neighborhood around p_1^0. Similarly, if p_1 lies outside of $\mathcal{B}$, then all points $p_1^0 + \alpha v_1$ also lie outside of $\mathcal{B}$.

For **case 1**, if both $\mathcal{M}_1$ and $\mathcal{M}_2$ are non-empty, then D^- is non-empty and connected. This will be shown by constructing a path between any two points, $q = (p_1, p_2) \in D^-$ and $q' = (p_1', p_2') \in D^-$. Let each point lie along a correspondingly named vector as in Fig. 4.

Points in D^- satisfy the following equation:

$$d(q)^2 = d_0^2 + d_0(r_1 v_1^z - r_2 v_2^z) + \mathcal{O}(\mathbf{r}^2) = d_0^2 - \epsilon + \epsilon^2 \tag{4}$$

This equation has a solution (near q_0 and for small ϵ) if either v_1^z is negative (i.e. $v_1^z \in \mathcal{M}_1$) or v_2^z is positive (i.e. $v_2^z \in \mathcal{M}_2$).

Start by assuming that both p_1 and p_1' lie in $\mathcal{M}_1$ and p_2 and p_2' lie in $\mathcal{M}_2$. To construct a path, denoted Γ, we start at (p_1, p_2) and move finger one, f_1, along v_1 to p_1^0. Eq. (4) can be solved for r_2, which is approximately linear in r_1, so f_2 may be moved along v_2 to maintain an interfinger distance of $d_0 - \epsilon$ during this motion. Move f_2 along v_2 to p_2^0, while moving f_1 along v_1' to maintain the interfinger distance. Finally, move f_2 along v_2' to p_2', while moving f_1 along v_1'. Finger one will arrive at p_1'.

Next, consider a point $q = (p_1, p_2)$ with $p_1 \in \mathcal{M}_1$ and $p_2 \in \mathcal{L}_2$. Move f_2 along v_2 to p_2^0 while moving f_1 along v_1. Denote this path β; its endpoint lies on path Γ. Any two points in D^- may be connected with combinations of paths β and Γ. Thus, if both $\mathcal{M}_1$ and $\mathcal{M}_2$ are non-empty, then D^- is connected and the sublevel sets of $\mathcal{F}$ do not change topologically at q_0.

For the remaining cases, either $\mathcal{M}_1$ or $\mathcal{M}_2$ is non-empty. Without loss of generality, assume that $\mathcal{M}_1$ is empty. Note that if $\mathcal{M}_1$ is empty, then $\mathcal{L}_1$ must be non-empty.

For **case 2**, if both $\mathcal{M}_1$ and $\mathcal{M}_2$ are empty, then D^- is empty, as (4) has no solutions. The fact that q_0 is an isolated point can be seen as follows: the only configurations containing $q = (p_1, p_2)$ that give $d(q) = d_0$ involve p_1 lying on $\mathcal{E}_1$, and p_2 lying on $\mathcal{E}_2$, exactly at the perpendicular projection of p_1 onto $\mathcal{E}_2$. Since non-generic parallel geometry has been excluded, this can only happen when $q = q_0$. Thus, q_0 is an isolated point.

For **case 3**, if $\mathcal{M}_2$ is disconnected, then D^- is disconnected and q_0 is a puncture grasp. This may be shown by contradiction. Assume D^- is connected; then there exists a path in D^- from $q = (p_1, p_2)$ to $q' = (p_1', p_2')$. Since $\mathcal{M}_2$ is disconnected, the path of f_2 must pass through $\mathcal{L}_2$. But $p_1 \in \mathcal{L}_1$ and $p_2 \in \mathcal{L}_2$ always results in $d(q) \geq d_0$, and cannot lie in D^-.

For **case 4**, if $\mathcal{M}_2$ is connected, then D^- is connected and q_0 is not a puncture point or immobilizing grasp. To show this we will construct a path in D^- between arbitrary points $q = (p_1, p_2) \in D^-$ and $q' = (p_1', p_2') \in D^-$. Choose r_1 and r_1' such that $p_1 = p_1^0 + r_1 v_1$ and $p_1' = p_1^0 + r_1' v_1'$. The path of finger one follows $p_1(s)$, as defined below.

$$p_1(s) = \begin{cases} p_1^0 + r_1(s) v_1 & : s \in [0, \frac{1}{2}] \\ p_1^0 + r_1(s) v_1' & : s \in (\frac{1}{2}, 1] \end{cases} \tag{5}$$

where $r_1(s)$ is chosen such that it varies from r_1 to zero over $s \in [0, \frac{1}{2}]$ and from zero to r_1' over $s \in [\frac{1}{2}, 1]$. Since $\mathcal{M}_2$ is connected, then there exists a path γ from p_2 to p_2', lying in $\mathcal{M}_2$, as shown in Fig. 5. Parameterize this path such that $\gamma(0) = p_2$ and $\gamma(1) = p_2'$. Consider a vector, $v_2(s)$, originating from p_2^0 that, for any s, passes through

$\gamma(s)$. Since $\gamma(s)$ lies outside of $\mathcal{B}$, then, by the geometric arguments above, all points $p_2^0 + r_2(s)v_2(s)$ lie outside of $\mathcal{B}$ for $r_2(s) \in (0, \delta)$. Solving (4) gives

$$r_2(s) = \frac{1}{v_2^z(s)}(r_1(s)v_1^z + 2\epsilon - \frac{1}{d_0}(\epsilon^2 - \mathcal{O}(\mathbf{r}^2)) \quad (6)$$

where v_1^z is the z-component of either v_1 or v_1'. Since both $r_1(s)$ and $v_2(s)$ are continuous, and $v_1^z, v_2^z > 0$, there exists a continuous positive solution for $r_2(s)$, for $s \in [0,1]$. Let $p_2(s) = p_2^0 + r_2(s)v_2(s)$. The path $q(s) = (p_1(s), p_2(s))$ connects q to q' and lies entirely in D^-. Thus, if $\mathcal{M}_2$ is connected then q_0 is not a puncture point or immobilizing grasp.

VIII. A Catalog of Immobilizing and Puncture Grasps

The above characterization gives a relatively simple way to categorize a double-contact point as an immobilizing grasp, puncture grasp, or neither. This section translates the above conditions into simple geometric tests that apply to most grasps. Section IX will analyze problem cases.

Definition 20: A double-contact configuration, $q_0 = (p_1^0, p_2^0)$, is **regular** if the following condition is met. Consider a point $q = (p_1, p_2)$ near q_0, such that a line segment joining p_1 and p_2 lies parallel to the grasp line. All such line segments must lie entirely within the object, $\mathcal{B}$, locally near p_1 and p_2.

Intuitively, *regular* grasps are those containing material between the finger contacts. The following geometric test may be used to evaluate a *regular* double contact $q_0 = (p_1^0, p_2^0)$. Consider the surface of $\mathcal{B}$ near p_1^0. Consider the interfinger distance of points near p_1^0 while keeping f_2 fixed at p_2^0, giving $d(p_1) = ||p_1 - p_2^0||$. Using this distance function, p_1 may be characterized as a local minima, a saddle, a local maxima, or none of these.

The contact pair $q_0 = (p_1^0, p_2^0)$ is an immobilizing grasp when $\mathcal{M}_1$ and $\mathcal{M}_2$ are both empty. This occurs when both contact points, evaluated with the other contact point fixed, are local minima. Thus, possible *regular* immobilizing grasps are shown in Fig. 6.

The contact pair $q_0 = (p_1^0, p_2^0)$ is a puncture grasp when $\mathcal{M}_1$ is empty and $\mathcal{M}_2$ is disconnected (or vice versa). This occurs when one contact point is a local minima and the other is a saddle, each characterized with the other point fixed. Possible *regular* puncture grasps are show in Fig. 7. Note that the saddle nature of contacts are drawn such that they divide a sublevel set into two disconnected regions: generically, the surface of a polyhedron may form saddles which divide sublevel sets into more than two connected regions, as in a monkey saddle.

IX. Sublevel Equivalence

The above algorithm assumed sublevel equivalence of free c-space, $\mathcal{F}$, and contact space, $\mathcal{U}$, as well as that of $\mathcal{U}$ and the caging graph, G. This section first shows the sublevel equivalence of $\mathcal{U}$ and G, using the convexity of the interfinger distance function. It then considers the case when sublevel equivalence of $\mathcal{U}$ and $\mathcal{F}$ fails, and shows that simple changes can restore sublevel equivalence of $\mathcal{U}$ and $\mathcal{F}$.

A. Sublevel Equivalence of $\mathcal{U}$ and G

The caging graph depends on the following decomposition of $\mathcal{U}$ having some useful properties.

Lemma 9.1: The function $d(\mathbf{s}) = ||p(s_1, s_2) - p(s_3, s_4)||$ is a smooth **convex function** in each contact-space polychoron.

Proof: Each contact-space polychoron, $\mathcal{P}_{ij}$, represents the placement of the fingers on two particular faces of $\mathcal{B}$. Consider the infinite planes underlying these faces. All non-parallel planes meet along a common line. Parameterize the position of a point on each plane as in Fig. 8, yielding $p_1 = (s_1, s_2, 0)$ and $p_2 = (s_3 \cos\theta, s_4, s_3 \sin\theta)$. The interfinger distance function can be written in these coordinates as $d(\mathbf{s}) = \left(\mathbf{s}^T K \mathbf{s}\right)^{\frac{1}{2}}$, where

$$K = \begin{bmatrix} 1 & 0 & -\cos\theta & 0 \\ 0 & 1 & 0 & -1 \\ -\cos\theta & 0 & 1 & 0 \\ 0 & -1 & 0 & 1 \end{bmatrix}$$

The eigenvalues of K are $\{0, 2, 1 \pm \cos\theta\}$, which are all non-negative. Thus K is positive semi-definite and $d(\mathbf{s}) = ||K^{1/2}\mathbf{s}||$. The function $d(\mathbf{s})$ is thus a composition of the Euclidean norm (a convex function) with the linear function $K^{1/2}\mathbf{s}$. Such a composition preserves convexity, and $d(\mathbf{s})$ is therefore convex in each polychoron, $\mathcal{P}_{ij}$. □

The next corollary follows from Lemma 9.1 and the definition of convexity.

Corollary 9.2: Let $\mathbf{s}$ and $\mathbf{s}'$ be two points on the boundary of a single contact-space polychoron, $\mathcal{P}_{ij}$. The straight line path between these two points lies in a single connected component of the c-sublevel set $\mathcal{U}_{\leq c}$ where $c = \max\{d(\mathbf{s}), d(\mathbf{s}')\}$.

Definition 21: A **c-sublevel set** of the caging graph G is the set of nodes, v, given by $G_{\leq c} = \{v(\mathbf{s}) \in G : d(\mathbf{s})) \leq c\}$.

The following theorem asserts that G preserves the sublevel connectivity of contact space, $\mathcal{U}$.

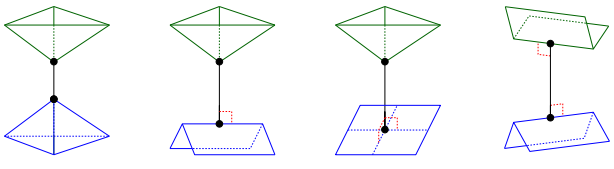

Fig. 6. A catalog of possible immobilizing grasps. Each contact represents a local minimum in the interfinger distance when the opposing finger is fixed.

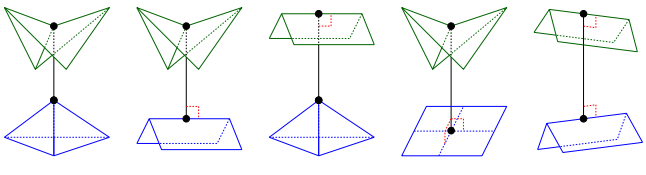

Fig. 7. A catalog of possible puncture grasps. Each contact represents a saddle in the interfinger distance when the opposing finger is fixed.

Theorem 2: The caging graph G is **sublevel equivalent** to contact space, $\mathcal{U}$. That is, there exists a path in $\mathcal{U}$ between two nodes $v_i, v_j \in G$, lying entirely in $\mathcal{U}_{\leq c}$, if and only if there exists a path along the edges of G between v_i and v_j lying entirely in $G_{\leq c}$.

Proof Sketch: For the forward direction, start with a path between two nodes, $v_i, v_j \in \mathcal{U}$, lying entirely in $\mathcal{U}_{\leq c}$. Divide this path into segments such that each segment lies in one contact-space polychoron. Next, replace each path segment with a straight line path between the segment's endpoints. By the convexity of $d(\mathbf{s})$ on the individual contact-space polychoron, the maximum value of $d(\mathbf{s})$ on each straight line segment is upper bounded by the value of $d(\mathbf{s})$ at its endpoints. The path connecting v_i and v_j is now piecewise linear. On each linear segment of this path, the value of $d(\mathbf{s})$ is still upper bounded by c according to Corollary 9.2. The two endpoints of each linear segment lie on the boundary of some polychoron $\mathcal{P}_{ij}$. Shift each endpoint to the minimum point of $d(\mathbf{s})$ along the same boundary edge of $\mathcal{P}_{ij}$, which is always a node of G. This local shifting can only *decrease* the value of $d(\mathbf{s})$ for that endpoint. The equivalent path in G thus lies entirely in the discrete sublevel set $G_{\leq c}$.

For the backwards direction, start with a discrete path between the nodes v_i and v_j lying entirely in $G_{\leq c}$. For each pair of adjacent nodes along the path, connect the two nodes by a straight line segment in $\mathcal{U}$. Each straight line segment lies in one polychoron, $\mathcal{P}_{ij}$. The maximum value of $d(\mathbf{s})$ along each segment is upper bounded by the value of $d(\mathbf{s})$ at either endpoint, per Corollary 9.2. The entire piecewise linear path thus lies in $\mathcal{U}_{\leq c}$. □

The following corollary is a direct result of Theorem 2.

Corollary 9.3: The caging graph G has the two properties:

1) The critical points of $d(\mathbf{s})$ in each connected component of $\mathcal{U}_{\leq c}$ correspond to a connected subgraph of G containing only the critical points lying in that component.
2) Every pair of sublevel sets of $d(\mathbf{s})$ in $\mathcal{U}$ that meet at a puncture point, $v \in \mathcal{U}$, correspond to two subgraphs of G that meet at the corresponding node, $v \in G$.

B. The Sublevel Equivalence of $\mathcal{U}$ and $\mathcal{F}$

To ensure sublevel set equivalence of $\mathcal{U}$ and $\mathcal{F}$, we must consider the topological changes which occur in each. Above we analyzed the topological changes at point $q_0 = (p_1^0, p_2^0)$ in free c-space, $\mathcal{F}$, based on the topology of two regions of $\mathcal{F}$, $\mathcal{M}_1$ and $\mathcal{M}_2$. Consider similar regions in $\mathcal{U}$, namely the intersection of the *boundary* of the polyhedron and the medial region, $\mathcal{M}$, around each of the finger placements.

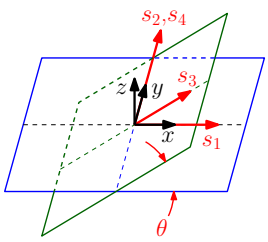

Fig. 8. A parameterization of two infinite planes, which demonstrates the convexity of $d(\mathbf{s})$.

Denote these regions $\mathcal{M}_1'$ and $\mathcal{M}_2'$. Note that $\mathcal{M}_i'$ is just the restriction of $\mathcal{M}_i$ to the boundary of $\mathcal{B}$.

The previous determination of the topology of $\mathcal{M}_i$ around contact points only assumes that if $p_1 = p_1^0 + r_1 v_1$ lies outside (or on the boundary) of $\mathcal{B}$, then $p_1^0 + \alpha v_1$ also lies outside (or on the boundary) of $\mathcal{B}$, for $\alpha \in (0, \delta)$. This assumption is true when restricting the fingers to the boundary of $\mathcal{B}$, so the resulting tests may be used to characterize $\mathcal{U}$ as well. Thus, if $\mathcal{M}_1'$ and $\mathcal{M}_2'$ are both empty, then at grasp q_0, an isolated point of $\mathcal{U}$ appears, which did not exist in $\mathcal{U}_{\leq d_0 - \epsilon}$, where $d_0 = d(q_0)$. This point would be an immobilizing grasp if finger motions were restricted to $\mathcal{U}$. If $\mathcal{M}_1'$ is empty and $\mathcal{M}_2'$ is disconnected, then at q_0, two (or more) regions of $\mathcal{U}$ which were disconnected in $\mathcal{U}_{\leq d_0 - \epsilon}$ join to form a connected component in $\mathcal{U}_{\leq d_0}$. This point would be a puncture grasp if finger motions were restricted to $\mathcal{U}$. If neither condition holds, then the topology of sublevel sets of $\mathcal{U}$ do not change at q_0.

We must now consider when the topology of sublevel sets of $\mathcal{U}$ and $\mathcal{F}$ change, and when those changes differ. Each region, $\mathcal{M}_i$ and $\mathcal{M}_i'$ may be either empty, connected, or disconnected. It can be shown that if $\mathcal{M}_i$ is empty, then $\mathcal{M}_i'$ is also empty, and that if $\mathcal{M}_i$ is disconnected, then $\mathcal{M}_i'$ is also disconnected. Thus, there are only two cases in which the topology of $\mathcal{M}_i$ and $\mathcal{M}_i'$ may differ: 1) $\mathcal{M}_i$ may be connected while $\mathcal{M}_i'$ is disconnected, or 2) $\mathcal{M}_i$ may be connected while $\mathcal{M}_i'$ is empty.

Adding the three cases where the topology of $\mathcal{M}_i$ and $\mathcal{M}_i'$ are the same (both empty, both connected, or both disconnected), there are five possibilities for the topology of the $\mathcal{M}_i$-$\mathcal{M}_i'$ pairs, resulting in 25 combinations when considering both contacts. Out of those 25 combinations, there are nine cases in which the topological changes of $\mathcal{F}$ and $\mathcal{U}$ differ, but these nine cases only take two forms, which we refer to as *false immobilizing grasps* and *false puncture grasps*. Both of these cases, and their effect on the sublevel equivalence of $\mathcal{U}$ and $\mathcal{F}$ will be considered in the following subsections.

Note that for a *regular* grasp at $q_0 = (p_1^0, p_2^0)$, each connected component $\mathcal{M}_i'$ is associated with exactly one connected component of $\mathcal{M}_i$, specifically the portion of free space located between that component of $\mathcal{M}_i$ and the boundary plane, $\mathcal{E}_i$. Thus, for a *regular* grasp, the topology change in $\mathcal{U}$ is the same as for $\mathcal{F}$ at every point.

C. Sublevel Equivalence at False Immobilizing Grasps

In a false immobilizing grasp, $\mathcal{M}_1'$ and $\mathcal{M}_2'$ are both empty, while either $\mathcal{M}_1$ or $\mathcal{M}_2$ is connected (or both). Thus, at q_0, an isolated point appears in $\mathcal{U}$, while no topological change occurs in $\mathcal{F}$. In $\mathcal{U}$, this appears to be an immobilizing grasp. The examples in Fig. 6 are false immobilizing grasps if the material lies above and below the contact points, rather than between them.

Consider the changes of topology in both $\mathcal{U}$ and $\mathcal{F}$ around a false immobilizing grasp at q_0. In $\mathcal{U}$, the sublevel set $\mathcal{U}_{\leq d_0 - \epsilon}$ is empty in a neighborhood of q_0. The sublevel set $\mathcal{U}_{\leq d_0}$ is the single point q_0, and $\mathcal{U}_{\leq d_0 + \epsilon}$ is a small

region around q_0. This cavity is isolated from other points in $\mathcal{U}$. There is no change in the topology of sublevel sets of $\mathcal{F}$ near q_0, and $\mathcal{U}$ and $\mathcal{F}$ are *not* sublevel equivalent. An isolated point appears in $\mathcal{U}$, but this point must lie in a connected component of $\mathcal{F}$ containing other double-contact points. The tunnel curve construction found below is essentially a constructive proof of this fact, and restores sublevel equivalence.

D. Sublevel Equivalence at False Puncture Grasps

In a false puncture grasp, $\mathcal{M}_1'$ is empty and $\mathcal{M}_2'$ is disconnected (or vice versa), while either $\mathcal{M}_1$ or $\mathcal{M}_2$ is connected. Thus, at q_0, two disconnected regions in $\mathcal{U}$ join, while no topological change occurs in $\mathcal{F}$. In $\mathcal{U}$, this appears to be a puncture grasp. The examples in Fig. 7 are false puncture grasps if the material lies above and below the contact points, rather than between them.

At a false puncture grasp, the changes in topology of $\mathcal{F}_{\leq c}$ and $\mathcal{U}_{\leq c}$ are qualitatively different, but sublevel equivalence still holds. At these types of grasp, two disconnected regions in $\mathcal{U}$ join at q_0, while the same regions are locally connected in $\mathcal{F}_{\leq d_0-\epsilon}$. However, if $\mathcal{U}$ and $\mathcal{F}$ are sublevel equivalent for $d(\mathbf{s}) = d_0 - \epsilon$, then the two regions must already be connected in $\mathcal{U}_{\leq d_0-\epsilon}$. As long as sublevel equivalence is not violated for interfinger distances smaller than $d_0 - \epsilon$, the changes in topology at q_0 will not violate sublevel equivalence.

E. Tunnel Curve Construction

To maintain sublevel equivalence between $\mathcal{U}$ and $\mathcal{F}$ at a false immobilizing grasp, we will add a *tunnel curve*, which is a path lying in $\mathcal{F}$ with endpoints in $\mathcal{U}$, to both $\mathcal{U}$ and G. This additional connectivity will guarantee that $\mathcal{F}$, $\mathcal{U}$, and G remain sublevel equivalent.

At a false immobilizing grasp, at least one finger can move away from object $\mathcal{B}$ in a straight line towards the other finger. Retract this finger while holding the other finger fixed on $\mathcal{B}$'s boundary, until the finger hits a new surface of $\mathcal{B}$. Both fingers now contact the object along its boundary. Slide both fingers simultaneously along the body while minimizing σ (i.e. squeeze the fingers), until reaching the unique minimum of the interfinger distance on these surfaces. This defines the tunnel-curve's endpoint. If, during the closing process, the fingers meet, the tunnel curve's endpoint is any escape point on the current contact-space polychoron. The start and end point of the tunnel curve are nodes of the caging graph, G. For each tunnel curve, add an edge to G connecting the nodes representing its endpoints.

The addition of these curves will restore the sublevel equivalence of $\mathcal{F}$, $\mathcal{U}$, and G, which may be seen as follows. The only points at which the topology of sublevel sets in $\mathcal{F}$ and $\mathcal{U}$ become different is at a false immobilizing grasp, when an isolated point appears in $\mathcal{U}_{\leq d_0}$, which is not isolated in $\mathcal{F}_{\leq d_0}$. Once a tunnel has been added to this point in $\mathcal{U}$ (and G), it is not isolated in $\mathcal{U}_{\leq d_0}$ (or G) when it appears.

X. Conclusion

This paper presented a new method to calculate the caging sets for a polyhedron by searching contact space rather than free space. The algorithm is based on two innovations. First, all critical points of the interfinger distance function were identified and characterized, resulting in a catalog of all immobilizing and puncture grasps. The critical points are nodes in a caging graph. Second, the relationships between 6D configuration space, 4D contact space, and the caging graph were analyzed, allowing a search of the caging graph. It was shown that contact space can be completely decomposed into 4D polychora, on which the interfinger distance is convex, allowing the relationship between contact space and the caging graph to be fully characterized. Additionally, the points at which the topology of sublevel sets of contact space and free configuration space differed were identified. The addition of edges to the caging graph reconciles these differences. An algorithm which searches the caging graph for puncture points of successively increasing interfinger distance was presented, and an example demonstrated the implementation of the algorithm.

References

[1] E. Rimon and A. Blake, "Caging 2D bodies by 1-parameter two-fingered gripping systems," in *Proc. IEEE Int. Conf. Robotics and Automation*, vol. 2, 1996, pp. 1458–1464.

[2] ——, "Caging planar bodies by one-parameter two-fingered gripping systems," *Int. J. Robot. Res.*, vol. 18, no. 3, pp. 299–318, 1999.

[3] A. Sudsang and J. Ponce, "On grasping and manipulating polygonal objects with disc-shaped robots in the plane," in *Proc. IEEE Int. Conf. Robotics and Automation*, vol. 3, 1998, pp. 2740–2746.

[4] J. Erickson, S. Thite, F. Rothganger, and J. Ponce, "Capturing a convex object with three discs," vol. 23, no. 6, pp. 1133–1140, 2007.

[5] P. Pipattanasomporn, P. Vongmasa, and A. Sudsang, "Two-finger squeezing caging of polygonal and polyhedral object," in *Proc. IEEE Int. Conf. Robotics and Automation*, 2007, pp. 205–210.

[6] A. Rodriguez, M. Mason, and S. Ferry, "From caging to grasping," *Proc. Robotics: Science and Systems*, 2011.

[7] A. Sudsang, J. Ponce, M. Hyman, and D. J. Kriegman, "On manipulating polygonal objects with three 2-DOF robots in the plane," in *Proc. IEEE Int. Conf. Robotics and Automation*, vol. 3, 1999, pp. 2227–2234.

[8] M. Vahedi and A. F. van der Stappen, "On the complexity of the set of three-finger caging grasps of convex polygons," in *Robotics: Science and Systems*, 2009.

[9] M. Vahedi and A. van der Stappen, "Caging polygons with two and three fingers," *Int. J. Robot. Res.*, vol. 27, no. 11-12, pp. 1308–1324, 2008.

[10] W. Wan, R. Fukui, M. Shimosaka, S. T, and Y. Kuniyoshi, "Grasping by caging: A promising tool to deal with uncertainty," in *IEEE Int. Conf. on Robotics and Automation*, 2012, pp. 5142–5149.

[11] ——, "A new grasping by caging solution using eigen-shapes and space mapping," in *IEEE Int. Conf. on Robotics and Automation*, 2013.

[12] P. Pipattanasomporn, P. Vongmasa, and A. Sudsang, "Caging rigid polytopes via finger dispersion control," in *IEEE Int. Conf. on Robotics and Automation*. IEEE, May 2008, pp. 1181–1186.

[13] P. Pipattanasomporn and A. Sudsang, "Two-finger caging of nonconvex polytopes," vol. 27, no. 2, pp. 324–333, 2011.

[14] T. F. Allen, E. Rimon, and J. W. Burdick, "Two-fingered caging of polygons via contact-space graph search," in *Proc. IEEE Int. Conf. Robotics and Automation*, 2012, pp. 4183–4189.

[15] J. Burkardt, "gourd.obj," September 2013. [Online]. Available: http://people.sc.fsu.edu/ jburkardt/data/obj/obj.html